A Short Review on Charge Packets and Space Charge Properties Inside Dielectrics

George E. Vardakis

Department of Electrical and Computer Engineering, Power Systems Laboratory, Democritus University of Thrace, Greece
gvarda@ee.duth.gr

Michael G. Danikas

Department of Electrical and Computer Engineering, Power Systems Laboratory, Democritus University of Thrace, Greece
mdanikas@ee.duth.gr

Zenon Achillides

Electricity Authority of Cyprus (EAC), Cyprus
zachillides@cytanet.com.cy

ABSTRACT

An effort to highlight the role of space charges inside dielectrics and their propagation is made in the present paper. Solid insulating materials in various parts of high voltage devices and machines are crucial for the insulating performance and their reliable functioning duration. Space charge distributions and space charge propagation in the form of pulses, called charge packets, are studied in this paper pointing out on one hand the initiating mechanisms and on the other hand the propagation mechanisms of charges inside dielectrics, as they are introduced in the scientific literature. Experimental data are used from other papers, mainly those referring to space charge distributions versus space and simultaneously versus time in a classification attempt of the aforementioned parameters.

I.   INTRODUCTION

The presence of space charges inside dielectrics is one of the most prominent indicators of defects and ongoing degradation processes of electrical insulation. As a high percentage of failures are associated with space charges, the need for the classification and evaluation of space charges is essential. Charge transport between electrode-dielectric interfaces were evaluated by measuring conduction currents in [1], and as further improvement to this technique, the Pulse Electroacoustic Method (PEA) was utilized to investigate space charge's profile distribution and transport inside the insulation. As an alternative to conduction current measurements, space Charge Packets (CPs) were introduced. CP analysis constitutes an important ageing factor for the solid insulation. CP is a net charge that remains in the form of a pulse as it crosses the insulation [2]. It has been observed that such packets can cause accelerated breakdown of insulation particularly when associated with continual charge accumulation. Authors in [3] firstly named the generation of packet-shaped SPs in 3-mm thick XLPE under 0.7 MV/cm = 70 kV/mm electrical field strength. CP initiation and propagation needs a strong theoretical background and analysis, for the charge injection, creation, propagation, and decay inside the polymeric insulation. Some of the most important mechanisms governed the CPs are mentioned below:

- Schottky emission (charge injection from metal to semiconductor/dielectric when the surfaces are in contact). For high fields electron energy (eV) is compared with the Schottky barrier φ.

- Fowler – Nordheim injection mechanism (tunneling) for low electric fields.

- Hopping conduction which is a very important mechanism for charge transport inside dielectrics (also called thermally assisted tunneling). This phenomenon corresponds to an intermediate situation whereby a trapped electron is brought by thermal activation to a level with the same energy to that of a neighbor site moving at this site by tunneling. There is discrimination in two cases.

- Conduction - Transport between trap sites charged when empty (Poole-Frenkel effect).

$$J \propto E e^{\frac{B\sqrt{E}}{k_B T}} \tag{1}$$

where J is the current density, B a constant, E the electric field, k_B the Boltzmann constant, and T the temperature.

- Conduction transport between trap sites that are neutral when empty:

$$J \propto \sinh\left(\frac{edE}{k_B T}\right) \tag{2}$$

with e is the electronic charge and d the distance between the traps.

- Trapping.
- Detrapping.
- Recombination depending to field and temperature.

The space charge accumulation may also be connected by:

- Charge ionization.
- Charge irradiation.
- Charge polarizations.

Figure 1 shows the conductions mechanisms in dielectric films. There is a clear discrimination between conduction between metal-dielectric surface (so called injection) and conduction inside the dielectric bulk [4].
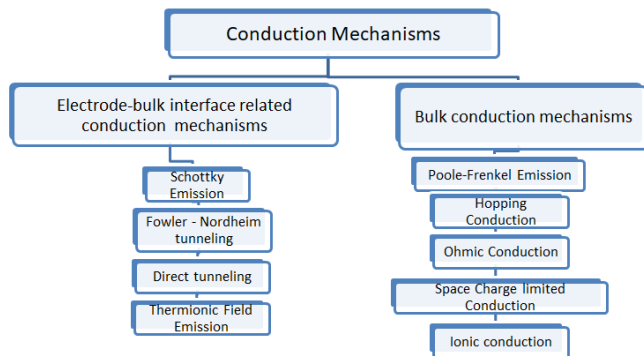

Fig. 1.   Classification of conduction mechanisms inside the dielectrics.

The basic set of equations for time-dependent diffusionless space charge flow for a single species of mobile charge carrier in a dielectric of constant relative permittivity ε are [5]:

$$\nabla J + \frac{\partial \rho}{\partial t} \tag{3}$$

$$J = \mu \rho E \tag{4}$$

$$\nabla E = \frac{\rho}{\varepsilon \varepsilon_0} \tag{5}$$

The transport equations (6) – (8) with the inclusion of a pair of oppositely charged species (electron and holes) are:

$$\frac{dJ(x,t)}{dx} + \frac{\partial(\rho_e + \rho_h)}{\partial t} = 0 \tag{6}$$

$$J = \left(\mu_h \rho_{h\mu} - \mu_e \rho_{e\mu}\right) E(x) \tag{7}$$

$$\frac{dE(x)}{dx} = \frac{\rho_e + \rho_h}{\varepsilon \varepsilon_0} \tag{8}$$

In order to describe more phenomena affecting charge propagation (conduction), one must take into account charge trapping, detrapping, and recombination (previously named annihilation). Charges, in the case of dielectric films, can be discriminated into four categories:

- Mobile electrons moving in conduction band.
- Mobile holes moving in valence band.
- Immobile electrons trapped in trap sites.
- Immobile holes trapped in trap sites as well.

Similarly to the aforementioned bipolar charge transport model, in [6], injection from both electrodes takes place following Schottky law with the relevant threshold electric field (barrier). It is evident in [6] that electrons from the cathode are injected to the conduction band with the Schottky injection mechanism and at the same time holes from the anode are injected to the valence band. The movements towards the electrode of the opposite polarity is defined and limited with phenomena such as trapping and detrapping at their relevant bands or at energy regions near their relevant bands. Recombination phenomena are also observed during their movement and propagation.

II.   CHARGE PACKET INITIATION

If the applied field exceeds the threshold field, then charge is injected from the electrodes inside the main insulating material and can be accumulated in traps located at the interface. Depending on the material, the applied voltage and the local electric field values, charge accumulation forms homocharges and sometimes heterocharges [7]. The notion of discrete pulse or charge generation in contradiction to the continuous charge generation is underlined in [2]. According to [2], a deeper understanding of electrode-polymer interface is needed, while a local production rate of charge must exhibit a form of hysteresis. Moreover, the low generation rate switches to a high rate, when a given local field is exceeded (similarly to the notion of a threshold field). The charges occur in front of the electrode, alter the electrical field, so the production rate reduces back to low when the modified electrical field is lower than the threshold field (or the threshold field changes its value due to the presence of the charge). The role of the aforementioned hysteresis loop [2] is intensified in [8], where the injection barrier alters its value under certain circumstances. The experimental data presented in [8] show the injection barriers varying between 1.2 eV and 1.3eV. The lower value leads to a high rate of charge injection reducing the local electric field from 160 to 115 kV/mm. After this reduction, the barrier height is restored again back to 1.3 eV decreasing the injection. The initiation and transport of large slow negative pulses was described in [9] by assuming field ionization in a three level system comprising an ionizable state, a trap state, and a valence band state. In this case, a plane of negative ionization is transferred through the system, as mobile holes released by the high field at the front of the plane move at the opposite direction to the plane and finally recombine with the ionized states at the rear of the plane.

III.   CHARGE PACKET PROPAGATION AND SPACE CHARGE DISTRIBUTIONS

Space charges are formed inside the main insulating materials when external electric stresses are applied to them. The Pulse Electroacoustic (PEA) method is a commonly used technique to acquire the profiles of space charge density ρ (Cb/m^3) versus the location (usually the distance between the electrodes). It must be emphasized that the PEA method and more specifically the PEA signal is very sensitive to the net charge at each point in the insulation bulk. Therefore, if positive and negative CPs (or charges generally) having similar amplitudes are injected simultaneously from both electrodes and overlap at a given point, then the detected PEA signal could show no charge profile (zero charge) at that particular point [7]. So, it is evident that a very difficult issue is the charge separation of positive and negative CPs. Temperature and more often time t are the parameters that are displayed in such profiles. Figures that show steady-state space charge distributions can be seen in [10-12]. The propagation of the above space charge profile from one electrode to the other is the definition of the CP. In [13], a positive charge accumulation is formed immediately after the voltage application in front of the anode with a peak value at 4×10^{-4} Cb/m^3 = 4×10^{-4} µCb/cm^3 space charge density. The sample is LDPE, pressed with PTFE (Polytetraflouroethylele), so called LDPE – F, whereas a -150 kV/mm DC voltage was applied to the sample. PEA is a method for space charge density calculation. After 10 min, the same profile is calculated. Positive space charge travels inside the insulating material, defining that a CP is a propagating accumulation of the space charge.

Based on the literature, a methodology is proposed for examining CP initiation:

- A negative charge approaching the anode, strongly enhances the electric field (heterocharge), which can cause the first positive CP in series.

- A new packet is formed upon the collapse of the old packet. The second CP is characterized by a high value for electric field in front of the packet (head) and a lower value behind it (tail).

- A third feature is that the positive CP leaves a negatively charged region when propagating. The background is the bipolar nature of transport, where positive and negative charges coexist in the same region.

- A fourth feature is the heterocharge buildup due to the transport of charges and their accumulation near the electrode of opposite polarity.

- The last feature is the weakening of packets, attenuating while propagating (dispersion and pulse widening. Others call this procedure decay).

An important parameter for studying the complex phenomenon of initiation and propagation of CPs is the mobility μ:

$$u = \mu \cdot E \qquad (9)$$

where u is the drift velocity (or migration speed), μ is the mobility, and E the mean electrical field. Several studies show that the charge mobility in insulating materials such as Polyethylene (PE) and Polypropylene (PP) has no-linear dependence on the local electric field. In [14], the samples were LDPE with 25 µm thick Polyvinyl Fluoride (PVF) films hot-pressed on both sides of the samples to prevent charge injection from the electrodes. Then the samples were irradiated with a 70 keV, 0.18 µA/cm^2 electron beam. After irradiation, a remarkable charge accumulation in a packet shape is found in the bulk of the sample near the surface of the irradiated side of the sample. Space charge profiles are acquitted in a time range of 0-390 s with repetitive time intervals for every measurement (almost every 30 s). Space charge densities vary from $\rho = -2$ µC/cm^3 = -2 C/m^3 to $\rho = +7$µC/cm^3, with a 30 kV/mm applied field.

Of course, in other publications and their respective experimental results, the charge profile does not show the same propagating characteristics. In [15], space charge density profiles in pure LDPE, at various values of external applied fields and temperatures show, as time t passes, alterations in their values but they do not show displacement or movements (no propagation happens) from the region where they initially appear. Some space charge distributions in [15] show that some peaks are sharper than others, but, as it is stated, the sensor position plays a crucial role at the measured accuracy. Moreover, scattering of the acoustic wave and attenuation are also important factors for these measurements. With applied fields of 30 and 50 kV/mm, space charge profiles are taken for 60 min with 10 min intervals. The resultant space charge profiles are shown in Table I.

TABLE I.   SPACE CHARGE DENSITIES, TIME AND APPLIED FIELD [15]

Material	Applied field	Time range	Temperature	Space charge densities	Remarks
LDPE	30 kV/mm		24 ºC	-20 to +20 µC/cm^3	No CP movements
LDPE	30 kV/mm	60 min (profile every 10 min)	50 ºC	-30 to +40 µC/cm^3	Slight CP displacement
LDPE	50 kV/mm		24 ºC	-30 to +35 µC/cm^3	No CP movements
LDPE	50 kV/mm		50 ºC	-15 to +35 µC/cm^3	No CP movements

In [16], the PEA is also utilized for the CP observation and moreover a Negative Differential Mobility (NDM), is found during CP propagation. The applied field is 20 kV/mm, with 100 µm distance between anode and cathode, the final subtracted space charge distribution results from -2 to +3µ C/cm^3. The used time for space charge measurements is 100 s.

In [7], the used specimens were cable models reproducing HV cables on a reduced-scale (mini-cables).The minicable consists of 2.8 mm conductor diameter, 0.7 mm inner semiconductor thickness and 1.5 mm XLPE thickness. The space charge profile patterns presented in [7] are distinguished into two categories. In the first category, the material is XLPE

mostly used in HV cables, whereas in the second case XLPE manufactured for MV is used. The polarization time is 10000 s for both cases, the applied electric strength value is 40 kV/mm, the used temperature is 25 and 70 ^{o}C, and the final space charge density varies from -10 to +10 μC/cm^3. It is evident from the space charge patterns of [7], that in the first case (XLPE HV cables), heterocharge is concentrated near each electrode and homocharges are shown in the second material (XLPE MV cables). In the first case, heterocharge build-up near both electrodes is noticed almost immediately at the beginning of the voltage application (polarization process). In the second case, it is noticeable that negative space charges are present near each electrode. In the case of the positive electrode, this space charge distribution establishes a heterocharge region whereas in the case of the negative polarity electrode this space charge distribution creates a homocharge region. In XLPE MV, a positive space charge pattern is formed almost at the central region of the insulating material. In [7], a positive charge packet propagates from the anode to the cathode in 0.5 s and after this a negative charge packet is shown travelling from the cathode to the anode in about 0.4 s (0.5-0.9). Of course, CPs of both polarities propagate simultaneously at the interelectrode area but for the sake of clarity these crosses are shown separately. Stationary Wavelet Transform (SWT) and initial profile subtraction were used for different purposes for acquiring space CP profiles. Temperature is a crucial factor for the aforementioned time durations. By increasing temperature, both positive and negative CPs are seen to move faster. In each case it is noticed that negative CPs travel faster comparing to positive CPs, as it is clear from the values in Table II.

TABLE II.   CP TRAVELLING DURATIONS DEPENDING ON THE TEMPERATURE [7]

	Positive CP	Negative CP
35°C	0.5 s	0.3 s
45°C	0.3 s	0.2 s
70°C	0.15 s	0.05 s

In [23], a simulation model is suggested for bipolar charge injection, transport, trapping, detrapping, and finally recombination effects. It is supposed that both electrons and holes are injected from the electrodes into the dielectric according to the Schottky law (injected carrier energy greater than the Schottky barrier). Charge trapping and detrapping effects in shallow traps are considered by a temperature dependent hopping type mobility μ as it is shown in (10):

$$\mu = \frac{2dv}{E(x,t)} e^{-\frac{ew_\mu}{KT}} \sinh\left(\frac{eE(x,t)d}{2KT}\right) \tag{10}$$

where d is the distance between the shallow traps, v is the attempt to escape frequency, T is the temperature, w_μ is the hopping barrier height for electrons and holes, and K is Boltzmann's constant.

IV. DISCUSSION

The experimental procedure can be discriminated into a low electric field and a high electric field as shown in Table III [16].

TABLE III.   HIGH AND LOW FIELD CHARACTERISTICS [16]

Low electric field	High electric field
E < 55 kV/mm	*E* > 55 kV/mm
No CPs are observed and only the normal space charge profiles are obtained by the PEA method. A bias DC voltage is utilized for the initiation of a CP, which is used as excitation method. A pulse voltage with a width of 250 ms and large amplitude of several kV is superimposed to the DC voltage.	A positive CP is formed without pulse excitation.
A CP (positive charge), is immediately formed (after the preceding excitation) at the anode and travels towards the cathode.	The CP appears 15 s after the voltage application.
The average velocity is evaluated and calculated from more than three measurements. It is first observed in PE. It resembles the "Gunn-Effect", seen in asemiconducting material [34]. It suggests that an NDM is involved in the behavior of positive charge carriers in PE in the case of low fields. According to the experimental findings, mobility can be evaluated for positive CPs and for low electric fields giving values (10^{-15}-10^{-14}) m^{2}V^{-1}sec^{-1}. Moreover, mobility tends to decrease when the field increases.	A decrease in velocity is observed as the field increases. Moreover, mobility calculation for the high electric field values shows that when increasing the electric field, the mobility decreases. In case of high electric field, similarly with the case of low electric field, NDM is noticed. Mobility depends on the electric field.

The relationship between the velocity of the holes and the applied field in polyethylene is demonstrated in [17]. It is noticed that the velocity of holes initially increases with the field and reaches its maximum value. After this peak, the velocity decreases, while *E* increases. In [14], the dependence of velocity versus the local electric field is obtained. A series of space charge migrations in LDPE are measured under a wide range of electric fields (15-50 kV/mm). In the same paper, the LIPP method (PEA method is the dominant procedure in the majority of scientific experiments) was used for the space charge distributions. A point of interest is that space charge injection was prevented by electrodes, via charge blocking layers, in order to define accurately the charges created due to

polarization and not from other sources (segregation from other sources).

After beam irradiation (maybe functioning as an excitation method), a remarkable charge accumulation of a packet shape, can be found in the bulk of the sample near the surface of the irradiated side of the sample. This CP gradually drifts to the opposite side maintaining its basic shape, consisting according to the definition a CP. The height of the CP gradually decreases due to the trapping effects. After calculations, the above curve shows that after 25 kV/mm, a negative differential region is found in accordance with the Negative Differential Resistivity (NDR) theory. A possible explanation is that mobility from (9) shows that the velocity is dependent on the electric field. The

resultant electrical field cannot be considered as uniform, due to the existence of the CP itself (e.g. a high concentrated charge region) which alters and modifies the electrical field or the resultant field is defined as the superimposition of the external and the local electric field. Additionally, in [13], LDPE was used, with different cooling rates and space charge distributions obtained with the High Voltage Withstand Pulse Electro Acoustic (HVW-PEA) method. Shortly, during the sample preparation, the lower cooling rates lead to a higher crystallinity degree. In three cases of cooling rates (high, medium, low) as the electric field increases (from 100 to 220 kV/mm), the mobility decreases. For values over 150 kV/mm, the mobility remains constant forming a plateau in all the three cases of cooling rates. In [18], it is shown experimentally that the launch of the first positive CP in the series happens when the negative charge front approaches the anode. A field enhancement in the region in front of the anode is responsible for the successive positive CP generation. Moreover, due to field dynamics, a high field corresponds to the front of the packet and a lower field behind it (tail). Another feature for the positive CP initiation and propagation is that the positive charge leaves behind it a negatively charged region according to the bi-polar charge transport, where positive and negative charges coexist in any location being only detected if a local unbalanced situation between them is established (the so called net charge). Authors in [7] however, define low CPs as the packets with mobility from 10^{-12} to 10^{-14} m^2/Vsec. In [7], the mobilities for positive and negative charges are calculated for the case of fast CPs. As it is evident from Table IV, mobility increases while the temperature increases, for both charge polarities. Furthermore, negative CPs demonstrate higher mobility values in comparison with positive CPs, at every temperature.

TABLE IV.   MOBILITY FOR FAST CPS. THERE IS A DISCRIMINATION BETWEEN POSITIVE AND NEGATIVE CHARGE CALCULATED AT EVERY TEMPERATURE [7]

	Mobility [m^2/Vs]		
	35°C	**45°C**	**70°C**
Positive charge	$7.2×10^{-11}$	$9.6×10^{-11}$	$1.9×10^{-11}$
Negative charge	$9.6×10^{-11}$	$1.4×10^{-11}$	$5.7×10^{-11}$

Moreover, in [19], for the separate estimation of positive and negative carrier mobility μ, a double layer experimental setup is used. The used barrier material has an extremely low conductivity and a high charge injection threshold compared with the testing material (LDPE or XLPE). For the experimental measurements held in [19], PTFE (Polytetrafluoroethylene) is used as the barrier material due to the aforementioned characteristics. PTFE was also reported in [13] for the same function.

As it is clear, when a DC voltage is applied between the upper and lower electrodes, carriers are injected from the upper electrode (carbon loaded polyethylene–semicon or SC) and, under certain circumstances, "travel" to the interface between the testing material and the barrier material. The charge buildup at the interface and the transport speed of carriers helps us for the mobility definition. Moreover, the choice of DC polarity allows us the calculation of positive and negative mobility. The PEA is also used for the time-dependent charge accumulation.

As it is mentioned in [5, 19, 20], the solution of the transport equation, the Poisson equation, and the continuity equation (6)-(8) will finally result in the mobility $\mu(t)$ as a function of time:

$$\mu(t) = \frac{2\varepsilon_2 d_2 \frac{dQ(t)}{dt}}{Q(t)(2\sigma_0(t) + \sigma_{if}(t) + Q(t))} \tag{11}$$

where $\sigma_0(t)$ is the surface charge density induced on the ground electrode, $\sigma_{if}(t)$ stands for the interface charges, and $Q(t)$ is the contribution of all the charges in the body of the testing material. Negative DC voltage is applied to SC electrode and the time-dependent space charge profiles are obtained (2 s, 20 min, 40 min, 60 min) for both PTFE/LDPE and PTFE/XLPE double-layer materials. Experimental data for both cases show that PTFE is an efficiently blocking material. Moreover, in the LDPE/PTFE interface, the accumulated charge is greater than the one at the PTFE/XLPE interface. This indicates that charge mobility in LDPE is greater than the mobility in XLPE.

The same results are obtained and in the case of positive DC voltage applied at the SC electrode. Charge accumulation is greater in the LDPE/PTFE interface than that in the XLPE/PTFE interface indicating higher mobility in the LDPE than in the XLPE sample. It is also found that the positive carriers move (slightly) faster than the negative ones. After relevant experiments, it has been found that in LDPE, the accumulated charge at the interface is mostly derived from the upper electrode (SC) through charge injection. Thus the contribution of intrinsic species must be neglected. Similarly, in [21], the field-dependent mobility is simulated versus the electric field. The mobility in [21] is the hopping mobility and the Gaussian Disorder Model (GDM) is used for hopping current estimation (negative charges, recombination effects, and traps). Similarly to the NDM presented above, in the case of hopping conduction, the simulated results clearly show that the mobility decreases as the electrical field increases. An explanation of this decrease is attempted in [21] considering a large amount of space charges moving inside the LDPE, consisting a packet-like. The positive charges accumulate due to the small number of hopping sited in the LDPE. In such a case, space charges move to the cathode and when the distance between them and the cathode shortens, additional space charges are injected from the anode in order to satisfy the constant potential condition. The velocity of the injected space charges is greater than the movement velocity of accumulated space charges due to the empty, vacant hopping sites. Thus, the injected charges are possibly in the form of CPs, and they reach immediately the accumulated space charge. The sudden increase of the accumulated charge leads to a decrease in velocity until the trap sites are fully occupied.

An increase in mobility for small electric fields is also stated in [22]. It was found that for high electric fields ($E > 90$ MV/m) CPs in the form of repetitive pulses transit the dielectric with a mobility from 10^{-16} to 10^{-14} m^2/Vs. According to [22], an unexpected outcome of the experiments was the observation of repetitive small charge pulses at lower electric fields (20-50 kV/mm) but having a mobility 4-5 orders of magnitude higher than the ones at high electric fields. In [22], positive and negative CPs are found propagating at the

interelectrode area, with total movement time of 1-1.5 s. Space charge density for CP pulses is -0.1 and +0.1 μC/cm³ for negative pulse and positive pulse, respectively, while the applied electric field is 30 kV/mm. Pulses of both signs show no attenuation or dispersion crossing the insulation with a mean mobility of 10^{-10} - 2×10^{-10} m²/Vs. The presence of these fast charge pulses was also experimentally observed not only with the PEA method but also with direct measurements of charging currents in XLPE cables in the same range of fields and temperatures. In addition, in [22], it is confirmed that space charge pulse mobility is a thermally activated mechanism, with 0.23 - 0.25 eV activation energy for positive pulses and 0.41 - 0.45 eV for negative pulses. These values are much smaller than those reported with XLPE, which are typically 1 eV or greater, corresponding to the deep traps that control and govern charge transport and the larger CPs travelling inside the dielectric in higher electric fields. The aforementioned values for mobility activation energy for XLPE are close to those of the mechanical relaxation (β and γ) of XLPE. This raises the possibility that local chain rearrangements associated with these relaxations are involved to the small pulse transport. Moreover, another characteristic of fast small CPs or pulses is that they remain coherent while passing through which results that their motion cannot be described by trap to trap transfer of the charges. Instead, their motion has the feature of a solitary wave, they seem to behave as solitons [22].

Table V summarizes the experimental results from 7 papers showing that LDPE is the dominant specimen used in space charge profile measurements. Moreover, electrical field ranges from 20 to 150 kV/mm and the distance between the anode and the cathode d is usually less than 0.6 mm. The various space charge profiles obtained at different time intervals are usually concluded within some minutes. Indicative space charge density values are demonstrated in the third column. It is evident from Table V that the dielectric material itself is one crucial parameter, so in Table VI, LDPE and their relative measurements are listed, similarly to Table V.

TABLE V. SUMMARY OF THE ELECTRIC STRENGTH APPLIED AT VARIOUS SPECIMENS. RELEVANT SPACE CHARGE DENSITY, TIME, AND ANODE-CATHODE DISTANCE ARE SHOWN

Ref.	E (kV/mm)	ρ (Cb/m³)	t (min)	d (mm)	Material
[12]	80	1.2	90	3.5	XLPE
[13]	150	400	10	0.1	LDPE-F
[13]	150	800	10	0.1	LDPE-G
[14]	30	7	6.3	0.5	LDPE
[15]	30	40	60	0.2	LDPE
[16]	20	15	6	0.1	LDPE
[20]	30.9	60	10	0.55	EPOXY-OP
[23]	50	30	60	0.25	LDPE

Figure 2 demonstrates the maximum value for space charge density ρ as a function of the mean electrical field E applied between the anode and the cathode only for LDPE. The small differences observed at the maximum space charge density values for identical mean electrical field values strength occur for a variety of reasons such as the manufacturing LDPE procedure which in not the same at various laboratories, the measurement duration which is listed in Table VI, and the

variety of the used electrode material. PEA is the utilized method in all cases. As expected, increasing E lead to space charge density increase, in the form of charge profiles or in the form of travelling CPs. Moreover, the local electric field, especially in front of each electrode, is a crucial quantity for space charge profiles.

TABLE VI. ELECTRICAL FIELD STRENGTH, SPACE CHARGE DENSITY, AND CONCLUSION TIME FOR PROFILE ACQUITTANCE ONLY FOR LDPE

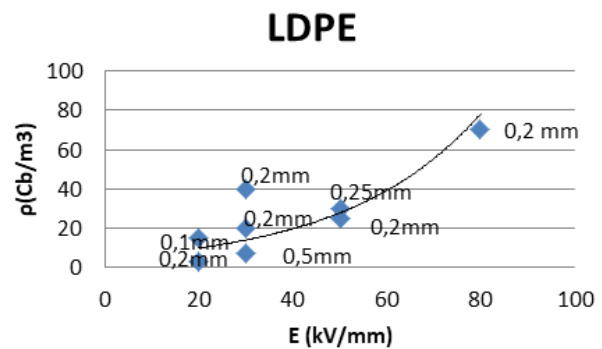| Ref.	E (kV/mm)	ρ (Cb/m³)	t (min)	d (mm)	Material
[16]	20	15	6	0,1	LDPE
[6]	20	3,5	120	0,2	LDPE
[1]	30	20	120	0,2	LDPE
[15]	30	40	60	0,2	LDPE
[14]	30	7	6,3	0,5	LDPE
[1]	50	25	120	0,2	LDPE
[23]	50	30	60	0,25	LDPE
[1]	80	70	120	0,2	LDPE

Fig. 2. For LDPE, maximum values of space charge densities versus mean electric field are shown. The parameters shown near each bullet correspond to the distance between anode and cathode.

In addition, Table VII and Figure 3 demonstrate that after the conclusion time for the final formation of CPs, the material itself plays an important role to the space charge density values.

TABLE VII. SPECIMENS AND THEIR SPACE CHARGE DENSITY VALUES AS A FUNCTION OF THE APPLIED ELECTRIC FIELD

Ref.	E (kV/mm)	ρ (Cb/m³)	t (min)	d (mm)	Material
[1]	80	70	120	0,2	LDPE
[20]	30,9	60	10	0,55	EPOXY-OP
[15]	30	40	60	0,2	LDPE
[23	50	30	60	0,25	LDPE
[1]	50	25	120	0,2	LDPE
[1]	30	20	120	0,2	LDPE
[16]	20	15	6	0,1	LDPE
[6]	20	4	120	0,2	DEGASSED XLPE
[6]	20	3,5	120	0,2	FRESH XLPE

The aforementioned admittance and experimental confirmation of fast CPs with very high mobility at relatively low electrical fields suits with the notion of Bruning's observations for charging phenomena in unexpected lower

values than that of the predefined thresholds. Yet on another question related to Bruning's consideration that charging phenomena are possible below the inception voltage (due to some minute irregularities on the cavity surface), there is some indirect confirmation in [13], where the morphology and the surface topography of polyethylene may affect space CP characteristics. Although the authors in [13] do not mention partial discharges and related phenomena, it is evident that surface treatment plays a role in determining CPs. In agreement with the above, in [24] it is noted that the formation of the packet-like charge is a result of a high conductivity region that is caused when traps are filled by electronic carriers (electrons or holes).
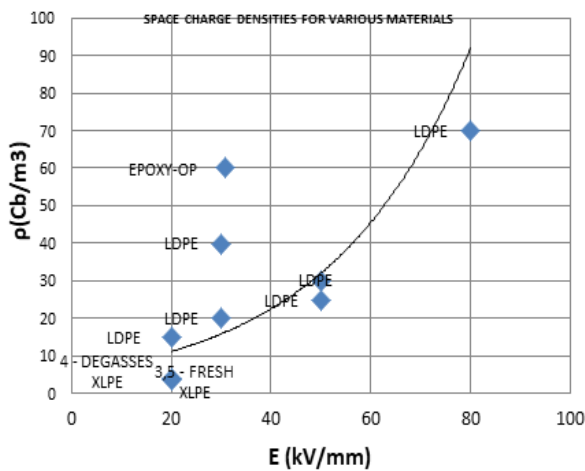

Fig. 3.   Space charge densities as a function of the applied electric field for various materials used as solid insulators.

In [25], various partial discharge models are presented. In all models, the role played by surface charge accumulation is evident. Furthermore, gas conductivity inside a cavity is also important [29, 30]. However, gas conductivity may appear even in the absence of partial discharges, conductivity which will not necessarily be "translated" (or transformed) into something detectable. Such ideas conform to [26], where it was reported that in minute cavities, partial discharges may have very long statistical time lag and the number of initial electrons may indeed be very small. In relatively low voltages, ionization processes of low energy may occur, which means that charges appearing in the cavity may result in clusters of space charges on the cavity walls. Such a space charge results in an electric field which – in the case of AC fields - is added to the applied electric field on the insulation [27]. Although what was described is the normal process of a PD, no one can exclude the possibility of having such events even below the inception voltage. The existence of space charges and partial discharges

inside the dielectrics plays a dominant role in the deterioration of their insulating capability. In [31-33], their contribution was analyzed, showing that these phenomena are present continuously in the HV industry and the related apparatus and the efforts to control and to study them may improve the HV apparatus reliability and insulation life time function. Charge packets propagation, space charges, partial discharges, electrical trees emanation and propagation, and electrical dipole formation are phenomena strongly correlated to each other, defining thus and affecting the insulating capability of materials.

A careful reader can observe that the whole approach of the space charge phenomena is related to the model proposed many years ago by Tanaka and Greenwood [28], namely that the electrodes, under AC conditions, inject and extract charges. Some electrons are emitted or injected into the dielectric during the negative half cycle for a short distance, limited by the declining stress away from the points. They will be drawn back into the point on the positive half cycle and re-injected in the following cycle. On each cycle, some of the electrons will gain sufficient energy to cause some polymer decomposition and thus create space charges in the bulk of the polymer. The estimated distance within which injected electrons can interact with the material to produce electrical trees near the tip of a needle is thought to be less than 20 μm. The tree initiation time (t) is related to the electric field (E), the effective work function φ (i.e. the difference between the work function of a metal and the electron affinity of a dielectric) with the following equation:

$$\ln t = \frac{B\varphi^{\frac{3}{2}}}{E} + \ln\left(\frac{C}{A}\right) \tag{12}$$

where A, B, and C are constants.

It must also be pointed out that a CP movement most of the times is observed with the aid of figures that show space charge densities versus space (usually the distance between anode and cathode) for various time intervals. That does not mean that every such profile can show CP movement. In [1], space charge profiles are obtained in LDPE samples for 30, 50, and 80 kV/mm versus time ranging from 0 to 7200 s. On the other hand, CPs of both signs travel from the anode to the cathode in LDPE when a 80 kV/mm field is applied [1]. The different time clearly demonstrates charge profiles constituted packet-like movements. At 0-120 s the negative injected charge is greater than the positive injected charge and a positive CP was found to be transported from the cathode to the anode. During the period from 120 to 300 s, negative CPs meet the positive ones near the anode where charge recombination occurs so a negative packet disappears (or better, overlaps), and a positive homocharge decreases by a great deal (partial overlapping must be taken into account).

TABLE VIII.   SPACE CHARGE DENSITIES, TIME, AND APPLIED FIELD [1]

Material	Applied field (kV/mm)	Time (s)	Space charge density (μC/cm³)	Remarks
LDPE	30	60, 200, 500, 1000, 1500, 2400, 7200	-8 to +20	No CP propagation. Slight charge shifts
LDPE	50		-17 to +25	
LDPE	80		-30 to +70	Charge packet propagation of both signs between electrodes.

V.   CONLCUSION

Space charge distributions and mainly charge packet propagation inside dielectrics are presented in this review paper. The mobility of both signs and charge packet propagation of both polarities are mostly shown and classified in the present work. There quantities are calculated and recorded over various materials at different specimen sizes with a variety of experimental setups utilized. The alteration of space charge distribution while time passes, enlightens the charge packet movement from one electrode to another. The charge packet initiation (and formerly injection) procedure is also presented, naming and underlining the physical mechanisms defining this phenomenon, accompanying with the relative set of equations. The relation of charge packets with previously published work on phenomena at and below the inception voltage is also indicated.

REFERENCES

[1]   Z. Lv, C. Zhang, Y. Ma, K. Wu, and Y. Cheng, "Analysis of the Charge Transport in LDPE with Combined Measurement of Space Charge and Current," in *3rd International Conference on Dielectrics*, Valencia, Spain, Jul. 2020, pp. 367–370, https://doi.org/10.1109/ICD46958. 2020.9341927.

[2]   L. A. Dissado, "The origin and nature of 'charge packets': A short review," in *10th IEEE International Conference on Solid Dielectrics*, Potsdam, Germany, Jul. 2010, pp. 1–6, https://doi.org/10.1109/ ICSD.2010.5568209.

[3]   N. Hozumi, T. Takeda, H. Suzuki, and T. Okamoto, "Space charge behavior in XLPE cable insulation under 0.2-1.2 MV/cm dc fields," *IEEE Transactions on Dielectrics and Electrical Insulation*, vol. 5, no. 1, pp. 82–90, Oct. 1998, https://doi.org/10.1109/94.660776.

[4]   F.-C. Chiu, "A Review on Conduction Mechanisms in Dielectric Films," *Advances in Materials Science and Engineering*, vol. 2014, Feb. 2014, Art. no. e578168, https://doi.org/10.1155/2014/578168.

[5]   J. M. Alison and R. M. Hill, "A model for bipolar charge transport, trapping and recombination in degassed crosslinked polyethene," *Journal of Physics D: Applied Physics*, vol. 27, no. 6, Mar. 1994, Art. no. 1291, https://doi.org/10.1088/0022-3727/27/6/029.

[6]   Y. Zhan *et al.*, "Space Charge Measurement and Modelling in Cross-Linked Polyethylene," *Energies*, vol. 13, no. 8, Jan. 2020, Art. no. 1906, https://doi.org/10.3390/en13081906.

[7]   D. Fabiani, G. C. Montanari, L. A. Dissado, C. Laurent, and G. Teyssedre, "Fast and slow charge packets in polymeric materials under DC stress," *IEEE Transactions on Dielectrics and Electrical Insulation*, vol. 16, no. 1, pp. 241–250, Feb. 2009, https://doi.org/10.1109/ TDEI.2009.4784573.

[8]   F. Baudoin, C. Laurent, S. Le Roy, and G. Teyssedre, "Charge packets modeling in insulating polymers based on transport description," in *Annual Report Conference on Electrical Insulation and Dielectric Phenomena*, Montreal, QC, Canada, Oct. 2012, pp. 665–668, https://doi.org/10.1109/CEIDP.2012.6378868.

[9]   K. Kaneko, T. Mizutani, and Y. Suzuoki, "Computer simulation on formation of space charge packets in XLPE films," *IEEE Transactions on Dielectrics and Electrical Insulation*, vol. 6, no. 2, pp. 152–158, Apr. 1999, https://doi.org/10.1109/94.765904.

[10] S. Wang, M. Fujita, G. Tanimoto, F. Aida, and Y. Fujiwara, "Decreasing space charge accumulation in polyethylene with an inorganic filler," *Journal of Electrostatics*, vol. 42, no. 1, pp. 219–225, Oct. 1997, https://doi.org/10.1016/S0304-3886(97)00150-2.

[11] S Tratteberg, E Idstad, R Hegerberg, "Influence of DC Voltage and Temperature Gradient on the Distribution of Space Charges in XLPE", *Nordic Insulation Symposium*, Tampere, June 11-13, 2003.

[12] M. Fu, L. A. Dissado, G. Chen, and J. C. Fothergill, "Space charge formation and its modified electric field under applied voltage reversal and temperature gradient in XLPE cable," *IEEE Transactions on Dielectrics and Electrical Insulation*, vol. 15, no. 3, pp. 851–860, Jun. 2008, https://doi.org/10.1109/TDEI.2008.4543123.

[13] Z. Yuanxiang, W. Yunshan, W. Ninghua, and S. Qinghua, "Effect of surface topography and morphology on space charge packets in polyethylene," *Journal of Physics: Conference Series*, vol. 183, no. 1, Dec. 2009, Art. no. 012009, https://doi.org/10.1088/1742-6596/183/1/012009.

[14] J. Meng, Y. Zhang, S. Hole, F. Zheng, and Z. An, "Charge mobility retrieval approach from apparent charge packet movements based on the negative differential resistance theory," *Scientific Reports*, vol. 8, no. 1, Apr. 2018, Art. no. 5928, https://doi.org/10.1038/s41598-018-24327-w.

[15] S. Akram, L. Ruijin, M. T. Nazir, and L. Yang, "Space Charge Characteristics of LDPE/MMT Nano-Composite Insulation Material under different Fields and Temperatures," *International Journal of Electrical & Computer Sciences*, vol. 12, no. 3, Jun. 2012.

[16] J. Zhao, G. Chen, and P. L. Lewin, "Investigation into the formation of charge packets in polyethylene: Experiment and simulation," *Journal of Applied Physics*, vol. 112, no. 3, Aug. 2012, Art. no. 034116, https://doi.org/10.1063/1.4745897.

[17] G. Chen and J. Zhao, "Observation of negative differential mobility and charge packet in polyethylene," *Journal of Physics D: Applied Physics*, vol. 44, no. 21, Feb. 2011, Art. no. 212001, https://doi.org/10.1088/ 0022-3727/44/21/212001.

[18] C. Laurent, G. Teyssedre, S. L. Roy, and F. Baudoin, "Charge dynamics and its energetic features in polymeric materials," *IEEE Transactions on Dielectrics and Electrical Insulation*, vol. 20, no. 2, pp. 357–381, Apr. 2013, https://doi.org/10.1109/TDEI.2013.6508737.

[19] R. Su *et al.*, "Investigation of effects of charge injection and intrinsic ionic carriers in low-density polyethylene and cross-linked polyethylene," *Journal of Applied Physics*, vol. 127, no. 16, Apr. 2020, Art. no. 165103, https://doi.org/10.1063/1.5142318.

[20] C. Cheng, K. Wu, R. Su, Y. Wu, and J. Dai, "A new method for carrier mobility measurement in oil immersed cellulose paper insulation," *IEEE Transactions on Dielectrics and Electrical Insulation*, vol. 26, no. 1, pp. 308–313, Oct. 2019, https://doi.org/10.1109/TDEI.2018.007733.

[21] K. Takeda, S. Yudate, R. Ozaki, and K. Kadowaki, "Numerical Simulation of Transient Behavior of Packet-Like Space Charge in Low Density Polyethylene," in *International Symposium on Electrical Insulating Materials*, Tokyo, Japan, Sep. 2020, pp. 327–330.

[22] G. C. Montanari, P. Seri, and L. A. Dissado, "Discovery of an unknown conduction mechanism in insulating polymers," *High Voltage*, vol. 5, no. 4, pp. 403–408, 2020, https://doi.org/10.1049/hve.2019.0355.

[23] F. Tian and C. Hou, "A trap regulated space charge suppression model for LDPE based nanocomposites by simulation and experiment," *IEEE Transactions on Dielectrics and Electrical Insulation*, vol. 25, no. 6, pp. 2169–2177, Sep. 2018, https://doi.org/10.1109/TDEI.2018.007282.

[24] Y. Ohki *et al.*, "Suppression of packet-like space charge formation in LDPE by the addition of magnesia nanofillers," in *9th International Conference on the Properties and Applications of Dielectric Materials*, Harbin, China, Jul. 2009, pp. 9–14, https://doi.org/10.1109/ICPADM. 2009.5252266.

[25] C. Pan, J. Tang, and F. Zeng, "Numerical modeling of partial discharge development process," in *Plasma Science and Technology: Basic Fundamentals and Modern Applications*, H. Jelassi and D. Benredjem, Eds. London, UK: IntechOpen, 2019, pp. 109–130.

[26] S. Avinash and K. Rajagopala, "Some Aspects of Stress Distribution and Effect of Voids Having Different Gases in MV Power Cables," *IOSR Journal of Electrical and Electronics Engineering*, vol. 5, pp. 16–22, Jan. 2013, https://doi.org/10.9790/1676-561622.

[27] S. M. Haque, J. A. A. Rey, and Y. Umar, "Electrical properties of different polymeric materials and their applications: The influence of electric field," in *Polymer Dielectrics: Properties and Applications of Polymer Dielectrics*, Rijeka, Croatia: IntechOpen, 2017, pp. 41–63.

[28] T. Tanaka and A. Greenwood, "Effects of Charge Injection and Extraction on Tree Initiation in Polyethylene," *IEEE Transactions on Power Apparatus and Systems*, vol. PAS-97, no. 5, pp. 1749–1759, Sep. 1978, https://doi.org/10.1109/TPAS.1978.354668.

[29] A. M. Bruning, D. G. Kasture, F. J. Campbell, and N. H. Turner, "Effect of cavity sub-corona current on polymer insulation life," *IEEE Transactions on Electrical Insulation*, vol. 26, no. 4, pp. 826–836, Dec. 1991, https://doi.org/10.1109/14.83709.

[30] M. G. Danikas and A. M. Bruning, "Comparison of several theoretical sub-corona to corona transition relations with recent experimental results," in *IEEE International Symposium on Electrical Insulation*, Baltimore, MD, USA, Jun. 1992, pp. 383–388, https://doi.org/10.1109/ELINSL.1992.246983.

[31] M. Danikas, G. E. Vardakis, and R. Sarathi, "Space Charges as Pre-breakdown Phenomena in Solid Dielectrics: A Concise Approach and Some Critical Comments," *Engineering, Technology & Applied Science Research*, vol. 10, no. 4, pp. 5992–5997, Aug. 2020, https://doi.org/10.48084/etasr.3667.

[32] G. E. Vardakis, M. Danikas, and A. Nterekas, "Partial Discharges in Cavities and their Connection with Dipoles, Space Charges, and Some Phenomena Below Inception Voltage," *Engineering, Technology & Applied Science Research*, vol. 10, no. 4, pp. 5869–5874, Aug. 2020, https://doi.org/10.48084/etasr.3593.

[33] M. Danikas, G. E. Vardakis, and R. Sarathi, "Some Factors Affecting the Breakdown Strength of Solid Dielectrics: A Short Review," *Engineering, Technology & Applied Science Research*, vol. 10, no. 2, pp. 5505–5511, Apr. 2020, https://doi.org/10.48084/etasr.3479.

[34] J. P. Jones, J. P. Llewellyn, and T. J. Lewis, "The contribution of field-induced morphological change to the electrical aging and breakdown of polyethylene," *IEEE Transactions on Dielectrics and Electrical Insulation*, vol. 12, no. 5, pp. 951–966, Jul. 2005, https://doi.org/10.1109/TDEI.2005.1522189.